



Aalborg Universitet

AALBORG UNIVERSITY
DENMARK

Analysis of a Computational Fluid Dynamics study on Seawave Slot-Cone Generator

Beseau, Maud

Publication date:
2006

Document Version
Tidlig version også kaldet pre-print

[Link to publication from Aalborg University](#)

Citation for published version (APA):
Beseau, M. (2006). *Analysis of a Computational Fluid Dynamics study on Seawave Slot-Cone Generator*.

General rights

Copyright and moral rights for the publications made accessible in the public portal are retained by the authors and/or other copyright owners and it is a condition of accessing publications that users recognise and abide by the legal requirements associated with these rights.

- Users may download and print one copy of any publication from the public portal for the purpose of private study or research.
- You may not further distribute the material or use it for any profit-making activity or commercial gain
- You may freely distribute the URL identifying the publication in the public portal -

Take down policy

If you believe that this document breaches copyright please contact us at vbn@aub.aau.dk providing details, and we will remove access to the work immediately and investigate your claim.

Peter Frigaard

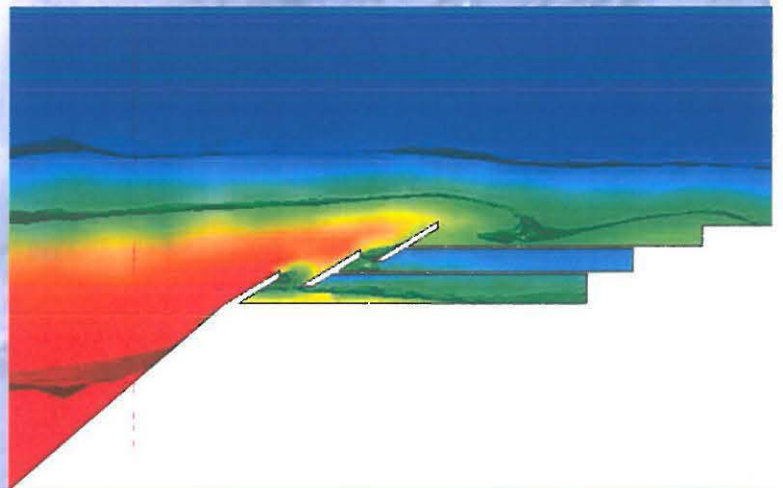

AALBORG UNIVERSITY



*Analysis of a
Computational Fluid Dynamics
study on
Seawave Slot-Cone Generator*

Maud Beseau, Aalborg University

June, 2006



Department of Civil Engineering

Aalborg University - Sohngaardsholmsvej 57 - DK 9000 Aalborg - Telephone +45 9635 8080



Acknowledgements

This project is not only the outcome of my efforts but constant guidance of many other people. Thus, I would like to thank my guides, Jens Peter Kofoed and Mickael Rasmussen, without whose support it would not have been possible to complete the work successfully.

I also express my gratitude towards others faculty members and students who made my stay a memorable one and a rich experience in Aalborg University.

Table of contents

- I. Introduction*
- II. Seawave Slot-cone Generator*
- III. Wave formation*
 - 1. Definition*
 - 2. Wave life*
 - 3. Wave hydrodynamics*
 - a. Basics equations*
 - b. Boundary conditions*
 - c. Linear or sinusoidal wave theory*
- IV. CFD software and CFX-10*
 - 1. Introduction*
 - 2. Computation Fluid Dynamics*
 - 3. CFX-10*
- V. Model SSG under extreme wave loading*
 - 1. Geometry*
 - 2. Mesh*
 - 3. Wave simulation*
 - 4. Solver*
 - 5. Results*
 - a. First computation: $H=0.38\text{m}$*
 - b. Second computation: $H=0.76\text{ m}$*
 - c. Rougher mesh with $H=0.38$*
 - d. Short model with $H=0.38\text{ meters}$*
 - e. Conclusion on the model simulations*
- VI. Full scale under extreme wave loading*
 - 1. Geometry*
 - 2. Mesh*
 - 3. Wave simulation*
 - 4. Solver*
 - 5. Results*
- VII. Full scale SSG with normal waves*
 - 1. Geometry and mesh*
 - 2. Wave simulation*
 - 3. Solver*
 - 4. Results*
- VIII. Conclusion*
- IX. References*

I. Introduction

The purpose of the study described in the present report has been to check the applicability of a Computational Fluid Dynamics (CFD) study concerning the wave loading induced on Seawave Slot-Cone Generator (SSG). Computational simulations with CFX-10 have been carried out in order to create extreme wave and to study the induced loadings on this wave energy converter.

Since CFD has met with difficulties to simulate wave, this study will specially analyze and evaluate the relevancy of the results. Thus different simulations have been needed to understand how the numerical approximations influence the results obtained. The result analysis will enable me to make some recommendations concerning CFD and wave simulations.

The first chapters present the SSG project and the wave theory. Then the next chapter will explain how CFD works and details about CFX are also presented. Finally the performed simulations are presented and their results are interpreted.

II. Seawave Slot-cone Generator

Traditional sources of energy such as oil, gas and coal cause pollution releasing huge quantities of carbon dioxide and other pollutants into the atmosphere. Nowadays, we can already see the caused damages such as global warming and climatic disorder. Moreover these energy sources are not renewable and their price is unstable, depending on international climate.

The Kyoto protocol regarding reduction of greenhouse gases is strictly linked to the development of Renewable Energy Sources (RES): wind, solar, waves and biomass. Wave energy has a great power potential: all over the Earth and the population is focused along the coast. In spite of technological difficulties due to the sea, different wave energy converters have been developing based on many principles such as overtopping, oscillating columns, buoys. In coming decades, it will be a challenge for engineers to generate electrical power from wave energy economically.

Seawave Slot-cone Generator (SSG), a wave energy converter (Fig.1), is developed by WAVEenergy AS company (Stavanger, Norway) founded in April 2004. This wave energy converter harvests the wave overtopping with three reservoirs placed on top of each other. The stored potential energy, the water captured in the reservoirs, will run through the multi-stage turbine and produce electricity (Fig.2).

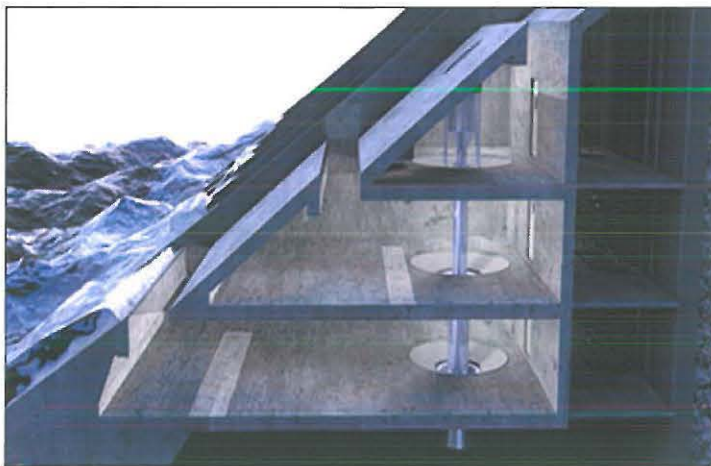


Fig.1: Scheme of Seawave Slot-cone Generator (SSG)

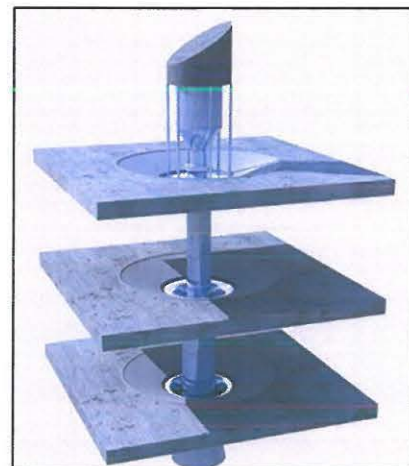


Fig.2: Multi-stage turbine

Partly founded by European Commission (WAVESSG project), WAVEenergy is carrying out a pilot project of the SSG at the island of **Kvitsoj** (Norway). The objective of this pilot project is to demonstrate at full-scale the operation of one module of the SSG in a 19 kW/m wave climate, including turbine, generator and control system and to connect the system to the public grid for electricity production. The pilot project regards a 10 m wide civil structure module of the SSG and will be installed within 2006.

The SSG can be integrated in a breakwater construction (Fig.3). So it will be able to have breakwater harvesting wave energy instead of usual breakwater. This may be a cost effective wave converter, utilising the foundation of the breakwater. The success of this concept will depend on the cost of its structure.



Fig.3: SSG integrated in a breakwater construction

III. Wave formation

1. Definition

A sea wave is a mechanical wave which propagates at the free surface between water and air. The wave displacement generates energy transfer and not mass transfer.

Therefore it is characterized by its period T , its wave length L , the water depth D , its speed $v=L/T$, its height $H = 2 A$ and its general shape $d = H/L$.

2. Wave life

If the wind reaches at least 4 knots on flat water surface, small oscillations are generated due to air displacement turbulence. Below this speed, the water surface tension prevents their formation. Then the waves grow up until they reach wind speed. Their growing up depends on fetch, wind speed and wind duration¹ (Table 1 and 2). The waves need space and time for reaching their maturity.

Wind duration (strength 7)	Wave height
3 hours	1 meter
6 hours	2 meters
12 hours	4 meters
20 hours	8 meters
24 hours	10 meters

Table 1: Influence of wind duration on wave height

Fetch (strength 7)	Wave height
20 miles	1 meter
100 miles	5 meters
300 miles	10 meters

Table 2: Influence of fetch on wave height

When the wind decreases, the waves continue their travel with few energy losses. Slowly, the gravity action will favour their spreading: the height decreases and the period and length increase.

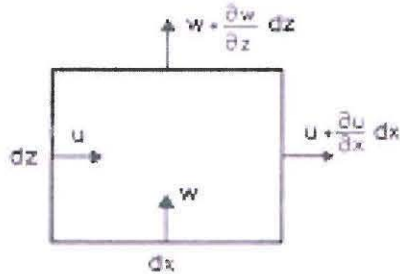
¹ Sverdrup, Norwich oceanographer

3. Wave hydrodynamics²

a. Basics equations

- Continuity equation

One of the most important physical principles is that mass is conserved in the fluid flow. Since water is incompressible, the conservation of mass becomes identical with conservation of volume: if the water is pushed, the water level increases. For a plane (x, y) finite control-surface, this principle is mathematically expressed by the **continuity equation**:



$$u dz + w dx = \left(u + \frac{\partial u}{\partial x} dx \right) dz + \left(w + \frac{\partial w}{\partial z} dz \right) dx \quad \Leftrightarrow$$

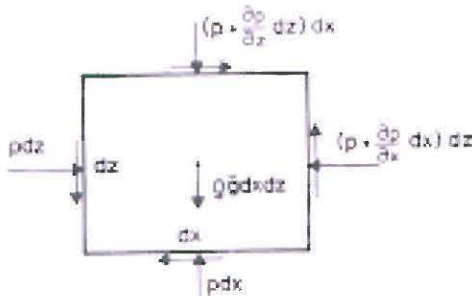
$$\boxed{\frac{\partial u}{\partial x} + \frac{\partial w}{\partial z} = 0} \quad (\text{Eq. 1})$$

Fig.4: Volume flow through fixed control-surface

- Momentum equations

Moreover, the fluid flow must satisfy **conservation of momentum**. When the water is high, the gravity results in the spreading. This motion will push the water and then the water level will increase.

That means Newton's second law must hold for any fluid particle: $m \frac{d\vec{v}}{dt} = \sum \vec{F}$ (Eq. 2)



There are three types of external forces acting on the fluid particle:

- normal forces: pressure
- shear forces: viscosity
- volume forces: gravity

Fig.5: Forces on a fluid particle

Then it is obtained:

Momentum equation in x-direction:

$$\rho \frac{\partial u}{\partial t} = - \frac{\partial p}{\partial x} + \text{viscous forces} \quad (\text{Eq. 3})$$

² A. Svendsen and G. Jonsson, *Hydrodynamics of coastal regions*, 1976

Momentum equation in z-direction:

$$\rho \frac{\partial w}{\partial t} = -\frac{\partial p}{\partial z} - \rho g + \text{viscous forces} \quad (\text{Eq. 4})$$

- Navier Stokes equations

However, since each fluid particle is moving it is not convenient mathematically to consider the accelerations of the individual fluid particles. Instead we want to describe the accelerations by the conditions at a fixed point.

Navier Stokes equations

$$\rho \left(\frac{\partial u}{\partial t} + u \frac{\partial u}{\partial x} + w \frac{\partial u}{\partial z} \right) = -\frac{\partial p}{\partial x} + \text{viscous forces} \quad (\text{Eq. 5})$$

$$\rho \left(\frac{\partial w}{\partial t} + u \frac{\partial w}{\partial x} + w \frac{\partial w}{\partial z} \right) = -\frac{\partial p}{\partial z} - \rho g + \text{viscous forces} \quad (\text{Eq. 6})$$

In our case, viscosity can be neglected and Euler equations can be used:

Euler equations

$$\frac{\partial u}{\partial t} + u \frac{\partial u}{\partial x} + w \frac{\partial u}{\partial z} = -\frac{1}{\rho} \frac{\partial p}{\partial x} \quad (\text{Eq. 7})$$

$$\frac{\partial w}{\partial t} + u \frac{\partial w}{\partial x} + w \frac{\partial w}{\partial z} = -\frac{1}{\rho} \frac{\partial p}{\partial z} - g \quad (\text{Eq. 8})$$

Three equations (Eq. 1, 7 and 8) has been stated; the unknowns are velocities in x-direction and z-direction and the pressures. For resolving these equations, the velocity potential has been used.

- Equations of potential flow

Under the following assumptions: conservative forces and inviscid fluid so irrotational flow, a scalar ϕ can be defined at each point of the flow in such way that the velocity $\vec{v} = (u, w)$ can

be determined as: $\vec{v} = \text{grad} \phi \Leftrightarrow (u, w) = \left(\frac{\partial \phi}{\partial x}, \frac{\partial \phi}{\partial z} \right)$

By replacing u and w by the velocity potential in the continuity equation, we obtain Laplace equation:

$$\boxed{\frac{\partial^2 \phi}{\partial x^2} + \frac{\partial^2 \phi}{\partial z^2} = 0} \quad (\text{Eq. 9})$$

By doing the same for Euler equations and by integrating, we obtain Bernoulli equation:

$$\boxed{\frac{p}{\rho} + gz + \frac{1}{2}(u^2 + w^2) + \frac{\partial \phi}{\partial t} = 0} \quad (\text{Eq. 10})$$

Now, the unknowns are p and ϕ . The solution of potential flow consists in solving the second order partial differential equation.

b. Boundary conditions

- Bottom conditions

The flow must be parallel to the bottom, expressed mathematically by $w=0$ at $z=-h$.

- Free surface conditions

On the free surface, a fluid particle will remain there.

Moreover the pressure is almost constant at the free surface, disregard the influence of wind, and since the density of air is 1/800 times smaller than water, we assume that $p=0$.

- Boundary conditions in x-direction, periodicity conditions

The conditions at the end of the region will determine the type of wave motion. In a case of a periodic progressive wave of constant form (propagates without change in form), we will have: $\phi(x,z,t) = \phi(x+L,z,t)$

c. Linear or sinusoidal wave theory

- Assumptions

- ✓ Constant depth D and period T
- ✓ Two-dimensional motion only
- ✓ Waves of constant form
- ✓ Incompressible fluid
- ✓ Effects of viscosity, turbulence and surface tension are neglected
- ✓ The general shape $\frac{H}{D} \rightarrow 0$

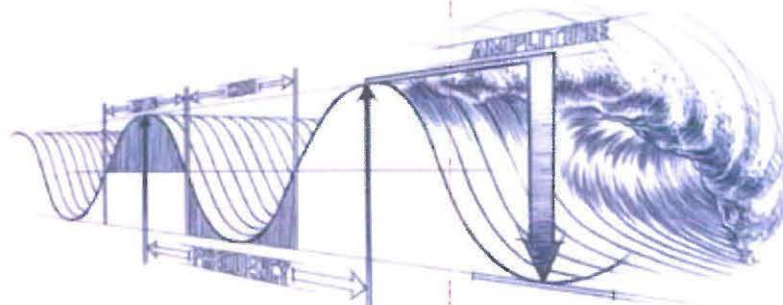


Fig.6: Perfect wave

- Solution for the velocity potential

Let $\theta = 2\pi \left(\frac{t}{T} - \frac{x}{L} \right) = \omega t - kx$

Then the Laplace equation (Eq.9) becomes: $k^2 \frac{\partial^2 \phi}{\partial \theta^2} + \frac{\partial^2 \phi}{\partial z^2} = 0$ (Eq. 11)

The problem can be solved by the method of separation of variables: $\phi(\theta, z) = f(\theta) \times Z(z)$.

Equation 11 becomes $k^2 f''(\theta)Z(z) + Z''(z)f(\theta) = 0$

$$\leftrightarrow -k^2 \frac{f''}{f} = \frac{Z''}{Z} = \lambda^2 \text{ where } \lambda \text{ is a constant.}$$

$$\leftrightarrow \begin{cases} f'' + \frac{\lambda^2}{k^2} f = 0 & \text{(Eq.12)} \\ Z'' - \lambda^2 Z = 0 & \text{(Eq.13)} \end{cases}$$

The solutions of these equations are: $f = A \sin\left(\frac{\lambda}{\theta} + \delta\right)$ and $Z = B \cosh(\lambda z) + C \sinh(\lambda z)$.

The constants A, B, C and λ can be found with the boundary conditions:

- Periodicity conditions: $f'(0) = f'(2\pi) \Rightarrow \lambda = k$
- At $z = -h$, $Z' = 0 \Rightarrow B = C \coth(kh) \Rightarrow Z = C \frac{\cosh(k(h+z))}{\sinh(kh)}$

Hence $\varphi(\theta, z) = -AC \frac{\cosh(k(h+z))}{\sinh(kh)} \sin(\omega t - kx)$ (Eq. 14)

- Surface profile

It is determined with the boundary condition: $\eta = -\frac{1}{g} \frac{\partial \varphi(\theta, z)}{\partial \theta} = -AC \frac{w}{g} \coth(kh) \cos \theta$

With the dispersion equation: $c^2 = \frac{g}{k} \tanh(kh)$ (Eq. 15), we obtain: $\eta = -\frac{AC}{c} \cos(\omega t - kx)$ (Eq. 16).

It is known that the wave amplitude is $\frac{H}{2}$ hence $-\frac{AC}{c} = \frac{H}{2}$.

Finally $\boxed{\eta = \frac{H}{2} \cos(\omega t - kx)}$ (Eq.17) and $\boxed{\varphi(\theta, z) = -\frac{Hc}{2} \frac{\cosh(k(h+z))}{\sinh(kh)} \sin(\omega t - kx)}$ (Eq.18)

- Velocity field

Once the velocity potential is obtained, the velocity field is found easily by derivation:

$$\begin{cases} u = \frac{\partial \varphi}{\partial x} = \frac{agk}{w} \frac{\cosh k(h+z)}{\cosh kh} \cos(\omega t - kx) & \text{(Eq. 19)} \\ w = \frac{\partial \varphi}{\partial z} = -\frac{agk}{w} \frac{\sinh k(h+z)}{\cosh kh} \sin(\omega t - kx) & \text{(Eq. 20)} \end{cases}$$

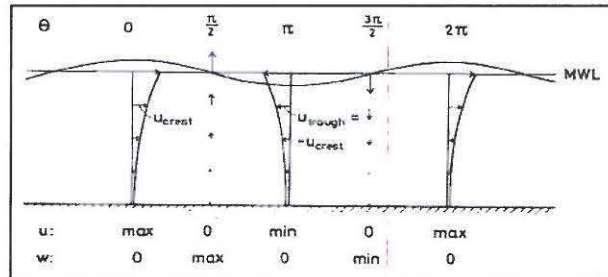


Fig.7: Velocity field

IV. CFD software and CFX-10

2. Introduction

The design of marine energy converter eventually requires the calculation of values such as pressure, motion amplitudes in order to assess the performance of the device and its suitability. Many programs have been devised to solve fluid dynamics problems of this nature, either specific or general application. Some programs have been produced by research departments mainly for in-house use; others have been developed commercially and are on general use.

In marine energy conversion applications, two main categories of software can be used: hydrodynamics software and computational fluid dynamics (CFD). In this study, a CFD software has been used: CFX-10.

The general nature of the CFD approach allows its application to many physical problem. Most of Fluid Dynamics Modelers cover many cases including both steady-state and transient, inviscid, laminar and turbulent flow in both incompressible and compressible fluids. Most provides the modeling of multiple-phase systems, often incorporating free surfaces between the fluids. The movement of the free surface can only be driven by pouring or 'sloshing' effects, or by penetration by another object. Hence the waves can not be defined exactly unlike with hydrodynamic software.

3. Computation Fluid Dynamics

The discretization of the three-dimensional model of the fluid domain entails the division of the volume into component cells. A grid of coordinate points (or nodes) is created within the fluid volume. A mesh is then generated using lines to connect the grids nodes thus forming edges of the component cells. Structured grids have a constant pattern of distribution of the nodes through space.

Before computation can take place, the physics regime must be defined. The model types of fluid, speed of flow, turbulence and viscosity must be chosen and parameters such as boundary and initial conditions set.

The CFD solver is based upon the full Navier-Stokes equations (Eq. 5 and 6), the Reynolds-averaged Navier-Stokes equations (RANSE) or the simplified inviscid flow Euler equations. The constituent partial derivatives of these equations must be discretized in time to enable a numerical solution to be found³.

The movement of the free surface is generally driven in one of two ways. The free surface can be set up in an initially unstable state and the model then predicts how the equilibrium is reached. Alternatively, the free surface can be driven by the movement of a boundary, such as a wall. This technique recreates a kind of wave maker for hydraulic laboratories.

Modelling of free surface is done in several ways, but the most frequently used in CFD is the Volume-Of-Fluid (VOL) method. This method assigns an extra identification variable, with

³ H.K. Versteeg & W. Malalasekera, *An introduction to Computational Fluid Dynamics*, Longman Group Ltd 1995

an associated transport equation, to each cell. The value of this variable designates to which fluid the cell belongs, and the cell boundaries where the value changes designates the position of the free surface. This method has the drawback of not being able to cope with non-linear effects like the breaking waves.

Unlike Fluent, Flow-3D, Phoenix and Star-CD, CFX uses a control-volume method. An extra variable assigns each cell: in hydrodynamics it will be Water Volume Fraction (WVF). The WVF varies between 0 and 1 and represents the percentage of water volume present in cells. It will be interesting to see the effect of this method on the results.

The results obtained from CFD calculation may be presented as time histories of forces, pressures, flows and temperatures. Visual data output may be produced as images as a fixed time point or as animations of the entire time history.

4. CFX-10

- Pre-processing

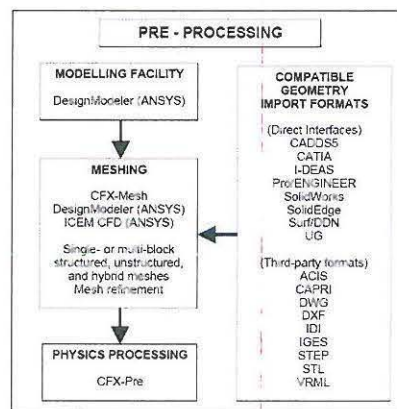


Fig. 8: Pre-processing

The DesignModeler for CFD Applications module provides geometry creation and meshing functions. Also geometry created with different design software can be imported. The CFX-Mesh program module has the capability of automatic surface and volume meshing. The program incorporates Advancing Front with Inflation (AFI) meshing technology. The volume meshing procedure is fully parallelized to accelerate the creation of large meshing. The procedure automatically fine-tunes the mesh spacing for areas where separate surfaces are in close proximity.

The CFX-Pre program module is an interface to permit the definition of the required CFD problem such as initialization, boundary conditions. When the problem is well-defined, a definition file is created to enable the solver to start the calculation.

- Computation

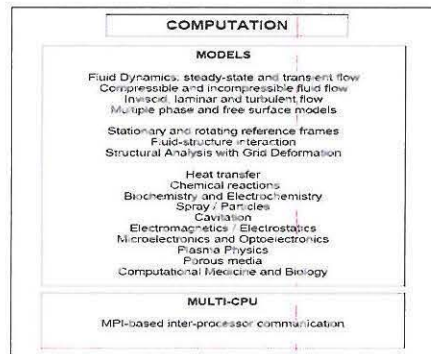


Fig. 9: Computation

CFX uses a coupled algebraic multi-grid Navier-Stokes equations solver, with an adaptive numeric scheme which modifies the discretization locally to approximate second-order problems as closely as possible. The solver does so with efficient utilization of the computer memory. The behavior of multiple phases is derived simultaneously using the coupled solver, which supports both Eulerian-Eulerian and Eulerian-Lagrangian multiphase models⁴. Free surface flow phenomena such as sloshing or filling can be simulated. The program also takes in account the surface tension effects.

Fluid-structure interaction simulations can be carried out. In the case of large-scale deformations or motions, CFX can be inter-connecting dynamically with ANSYS stress analysis and dynamics programs. CFX software has a strong history in the analysis of rotating machinery such as pumps, compressors, turbines or propellers.

The solver has been designed to be fully parallel to distribute the CFD calculation among several processors or networked UNIX workstations and Windows NT machines.

- Post-processing

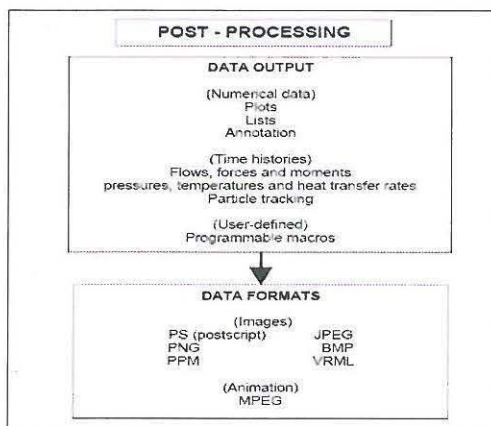


Fig. 10: Post-processing

The CFX-Post program module performs the 'Post-processing' functions for CFX-10. Results can be animated with automatic MPEG-format file creation. The program also performs quantitative calculations such as force, pressure and flow rate on a selected face.

⁴ A.P. McCabe, *An Appraisal of a Range of Fluid Modelling Software*, Department of Engineering Lancaster University, October, 2004

V. Model SSG under extreme wave loading

Wave loading experiences has been done by Diego Vicinanza at the hydraulic and coastal laboratory of Aalborg University⁵. The aim of the experience was to help the structure designers on wave loading acting on different parts of the structure. A model of SSG at scale 1:60 was used for the experiment. In these computations, the same dimensions have been employed.

1. Geometry

The dimensions of the model geometry are presented below:

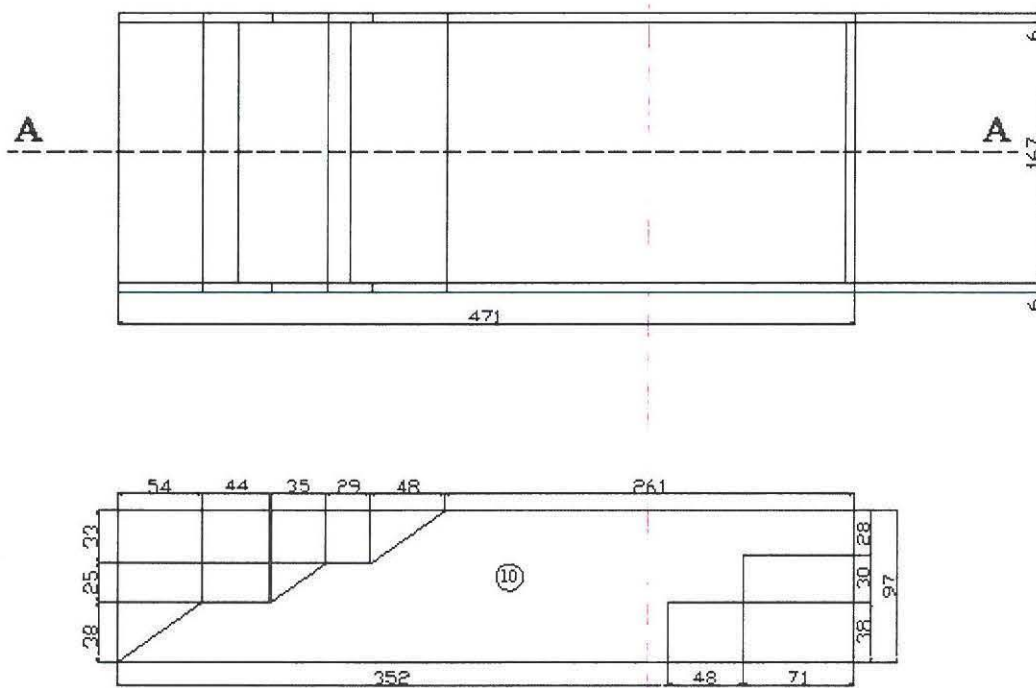


Fig. 11: Dimension of the model structure geometry

The structure has been modeled with ANSYS Workbench and the modelization did not require a lot of time because of the simple geometry. The fluid domain has to be long to enable the waves to form themselves, a length of 11 m has been chosen. The height of the fluid domain is 1 m and the mean water level will be initialized at 0.5 m. Once a 2D model has been drawn in a plane, the model is extruded of 0.5 m on the z-direction.

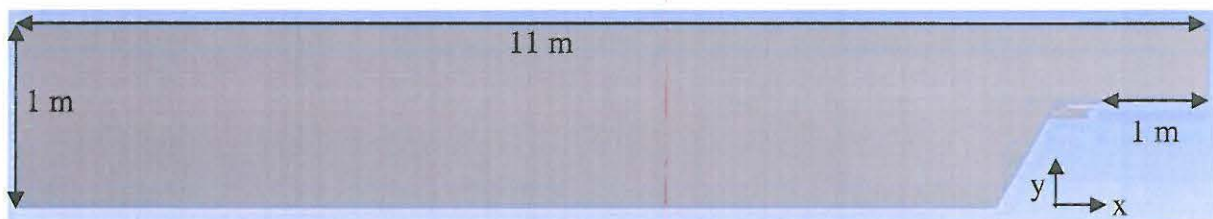


Fig.12: Geometry of the model in ANSYS Workbench

⁵ Diego Vicinanza et al., Wave loadings on Seawave Slot-Cone Generator at Kvitsøy Island, Hydraulics & Coastal Engineering Laboratory, Aalborg University, March 2006.

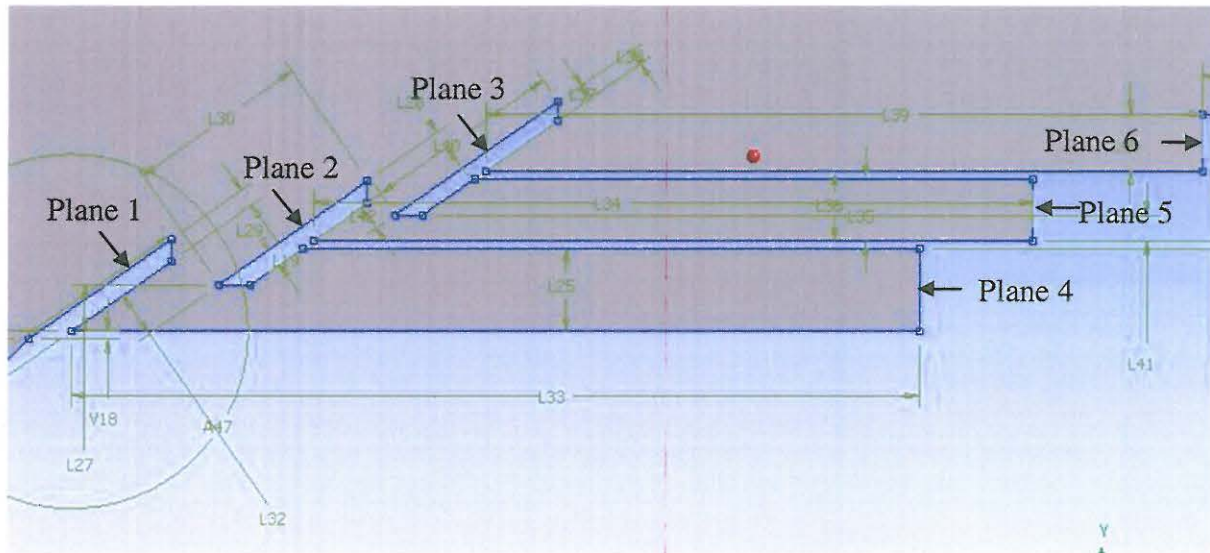


Fig.13: Detail of SSG geometry in ANSYS Workbench

2. Mesh

Mesh has been defined as follows:

Body spacing	Maximum spacing	70 mm
Face spacing (Plane 1 to 6)	Maximum spacing	5 mm
	Minimum spacing	10 mm

Table 3: Mesh spacing

The mesh spacing has been reduced on plane 1 to 6 in order to have a better accuracy of the results concerning pressure. Finally, the grid is composed by 43577 nodes and 214573 tetrahedron elements.

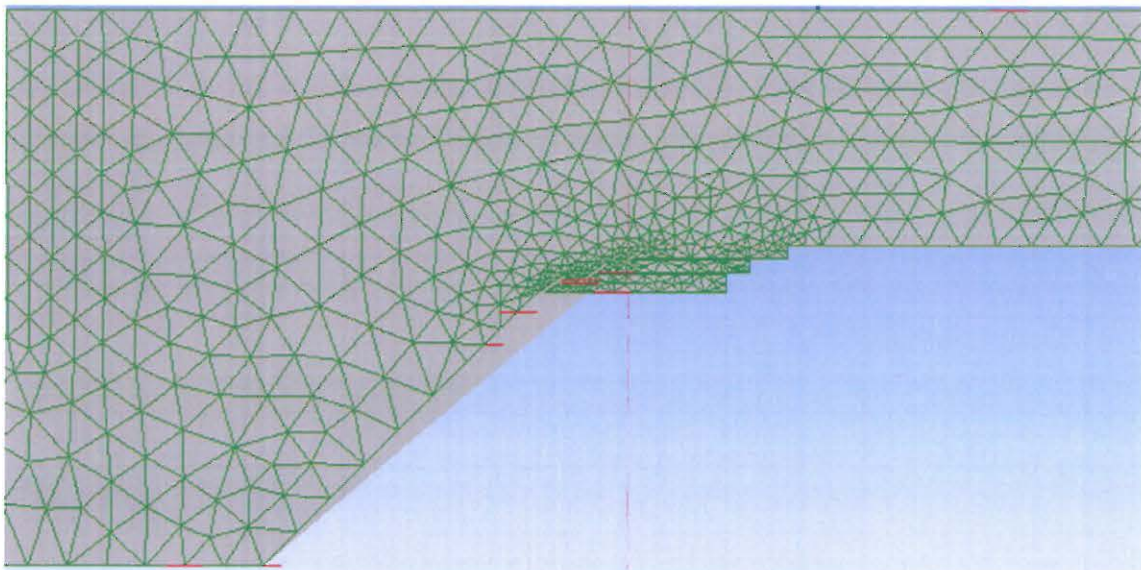


Fig.14: Mesh around the model of SSG

The figure 14 shows mesh is finer around the Model. However, the fluid domain around mesh is rough in order to reduce computational time and memory.

3. Wave simulation

The structural design of SSG must be based on this extreme wave. The computation will be performed in order to know the pressure generated by extreme waves. For head-on waves the 100 year event at prototype site can be given by wave condition $H_s=12.5$ m and $T_p=15.2$ s, based on the study by Nygaard and Kenneth (2002). Hence it is deduced that $H_{100}=23.3$ m and $T_{100}=12.3 - 16$ s. At scale 1:60, the experimental wave condition was $H_s=0.21$ m and $T_p=1.98$ s hence it has been used $H_{100}=0.38$ m and $T_{100}=1.98$ s.

From the wave condition, wave parameters have been calculated. Wave length is computed with the dispersion equation (Eq. 15) and the water velocity profile is calculated with Eq. 19

Parameters	Formulae	Values
Wave length L	$c^2 = \frac{g}{k} \tanh(kh)$	4 m
Wave number k	$\frac{2\pi}{L}$	1.57
Period number w	$\frac{2\pi}{T}$	3.17
Propagation speed v	$\frac{L}{T}$	2 m/s
Velocity profile	$u = \frac{agk}{w} \frac{\cosh k(h+z)}{\cosh kh} \cos(\omega t - kx)$	$u = 0.7 \cosh 1.57(0.5 + z) \cos(3.57t - 1.57x)$ (Eq.21)

Table 4: Wave parameters

In the simulation, the water level has been initialized at 0.5 m (Fig.15). Under this height only water is present: Water Fraction Volume = 1, represented with red, and above only air is present: Water Fraction Volume = 0, represented with blue.



Fig.15: Water level initialization

Then, boundary conditions (Fig.16) have been defined in the fluid domain:

- Inlet for the front wall
- Opening for the top
- Outlet for the back wall
- Symmetry for the side walls (so it is not needed to have a large model)
- Walls everywhere else (SSG and bottom)

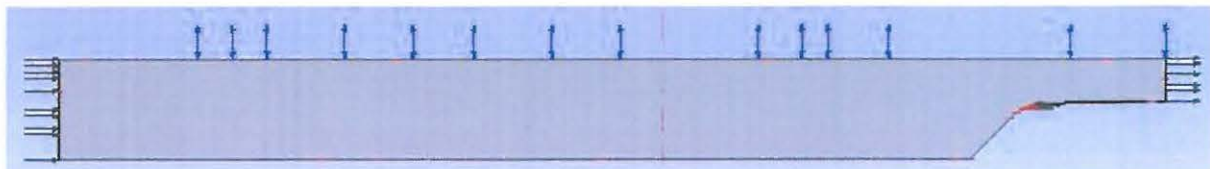


Fig.16: Boundary conditions

For simulating waves in CFX, the velocity field at the inlet has been defined with the equation 19 that becomes at the inlet ($x = 0$): $u = 0.7 \cosh 1.57(0.5 + z) \cos(3.57t)$ (Eq.22).

To define the inlet and initialization conditions, the following expressions have been written in CFX-Pre:

Variables	Name	Formulae
Density	Dens	998 [kg m ⁻³]
Wave height initialized	H	0.5[m]
Wave height at the inlet	HIn	0.69[m]
Pressure at the inlet	InPres	dens*g*(HIn-y)*InVolWater
Speed at the inlet	InSpeed	0.7*cosh(1.57*Xsd)*cos(3.17*time)*InVolWater [m/s]
Air Volume Fraction at the inlet	InVolAir	step((y-HIn)/1[m])
Water Volume Fraction at the inlet	InVolWater	1-InVolAir
Initialized pressure	pression	dens*g*(H-y)*VolWater
Time variable dimensionless	time	t/1[s]
Initialized Air Volume Fraction	VolAir	step((y-H)/1[m])
Initialized Water Volume Fraction	VolWater	1-VolAir
Height variable dimensionless	Xsd	y/1[m]

Table 5: Expressions used in CFX

The step function enables to define the air and water volume fraction. The InSpeed corresponds to water particle velocity so in a cell full of air the fluid velocity is null. Therefore the speed at the inlet depends on these volume fractions.

The water particle velocity depends on time; it is either positive or negative. Therefore the water volume is constant during one wave period. A river would have been simulated if the water velocity would have been constant.

4. Solver

The simulation is transient and has used a time step of 0.099 seconds; hence there are 20 time steps per period. The simulation covers 5 wave periods (9.9 seconds). A transient output file has been created every 2 time steps (0.198 seconds). These output files will enable to watch results step by step, to present them as time history and to make an animation.

The selected transient scheme option is first order backward Euler for saving computational time. Between each time step, 10 loops are done for converging it.

5. Results and interpretations

a. First computation: $H=0.38\text{m}$

An animation has been made with all transient files and the wave formation and displacement can be observed. Firstly, it has been observed that the waves are damped during their displacement. The wave defined at the inlet does not keep its height (Fig.17). The extreme wave is just like a normal wave in front of SSG.

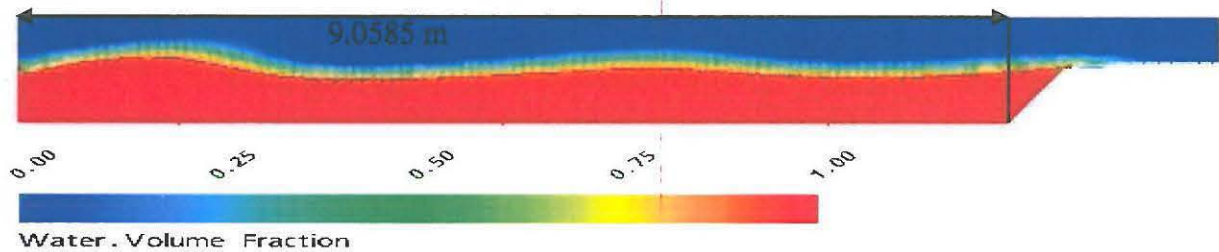


Fig. 17: Water volume fraction after 8.514s

In order to know the wave height before the SSG, the water level has been reported for every 2 time steps on the plane $x = 9.0585\text{m}$. The water level has been defined when the water volume fraction is equal to 0.5, so when the volume element is composed of half water and half air.

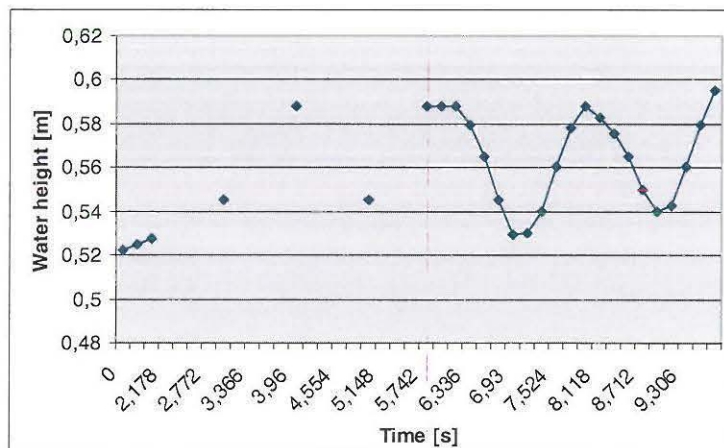


Fig. 18: Water level time history on the plane $x = 9.0585\text{m}$

The observations are:

- The maximum wave height is around 0.059 meters (0.588 m - 0.529 m).
- The mean water level increases and reaches 0.56 meters.

At the inlet, the wave height was 0.38 meters and after 9.085 meters it is only 0.059 meters. There is a ratio 6.44 between the both wave heights. The waves, which arrive at SSG, represent waves of height 3.54 meters at scale 1:1 instead of height of 23 meters as desired.

In CFX-Post, the average of the pressure on a face can be calculated by using the function calculator. The averaged pressures on the front and back walls of SSG (plane 1 to 6) have been recorded and plotted as function of time (Fig.19).

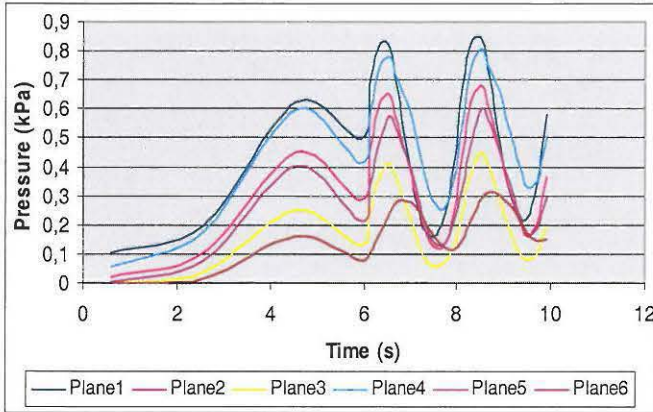


Fig. 19: Pressures time history on SSG's walls

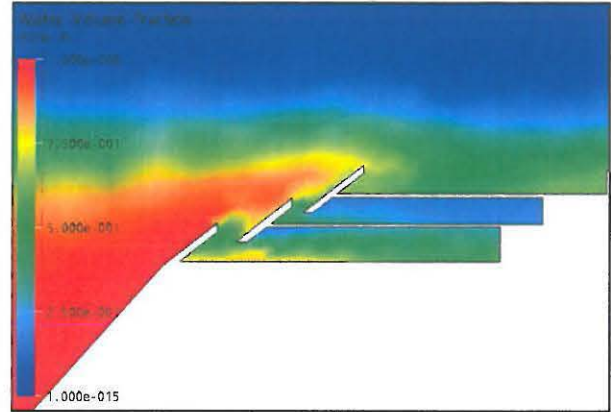


Fig. 20: WVF after 8.514s (peak pressure)

The maximum pressure is 0.836 kPa which corresponds to the Froude scaled pressure value of **50.16 kPa** at real scale.

All the front walls of reservoirs are more loaded than the back walls. The lowest reservoir is the most loaded and then it is the middle reservoir. Higher the reservoir, lower the water flow, so the pressure generated is less significant. The lowest reservoir is subject to the greatest pressure (Fig. 20).

The wave height is damped with a factor 6.44 during the wave propagation. It would be interesting to see what the effect of increasing the wave height at inlet. The next computation has been done by changing only one parameter: the wave height ($H=0.76\text{m}$). The same geometry, meshing and problem definition have been used.

b. Second computation: $H=0.76\text{ m}$

The wave height has been changed only. Then the velocity profile (Eq.21) at the inlet becomes at the inlet ($x = 0$): $u = 1.39 \cosh 1.57(0.5 + z) \cos(3.57t)$ (Eq.23). By doubling the wave height, the velocity amplitude is multiplied by two. Moreover the general shape of wave, ratio between the height and the length, is modified and equal to 0.19 ($>1/7$) which means that is a breaking wave.

The Water Volume Fraction (WVF) has been presented on the figure 20.

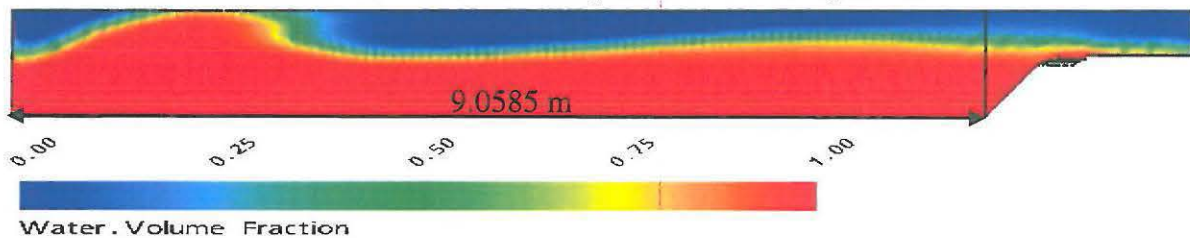


Fig. 21: Water Volume Fraction after 8.514s

The wave shape has been modified compared with figure 17 and a breaking is observed at the beginning of the fluid domain. Then the wave height is damped and the water level seems to increase. From the beginning of the slope, the layer, where the Water Volume Fraction varies between 0.25 and 0.75, becomes larger

The water level, defined when WVF=0.5, at plane $x = 9.0585$ m plotted in the figure 22 confirms this observation.

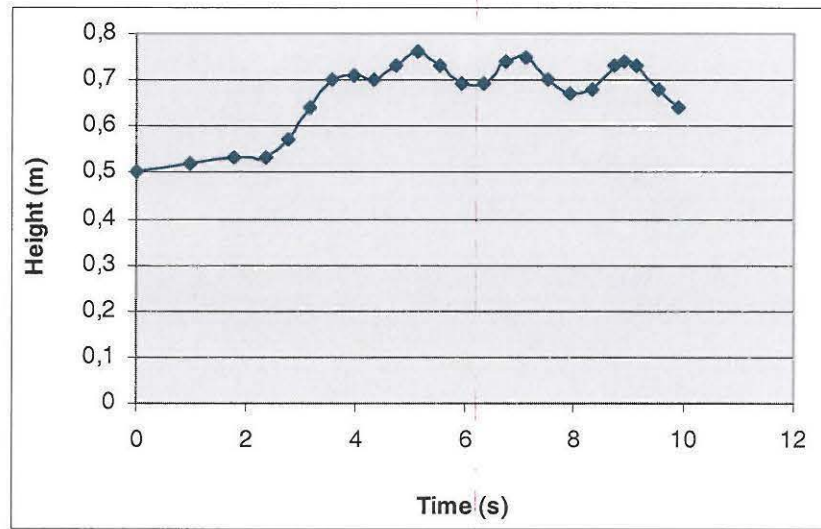


Fig.22: Water level time history at $x = 9.0585$ m

A maximum wave height of 0.08 meters has been calculated. At scale 1:1, such wave corresponds at a wave of height 4.8 meters. Even if the wave height at the inlet has been doubled, the wave height before the slope has slightly increased. The mean water level has increased again and reaches 0.7-0.71 meters. Therefore by increasing the wave height at the inlet, the water level improves in front of SSG. Instead of a clear interface between water and air, a diffusion of water is observed: on a height of about 0.2 m, the Water Volume Fraction is around 0.5.

The pressure time history is presented in the figure 23:

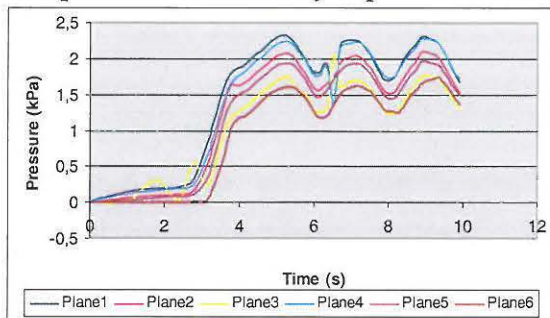


Fig.23: Pressure time history on SSG walls

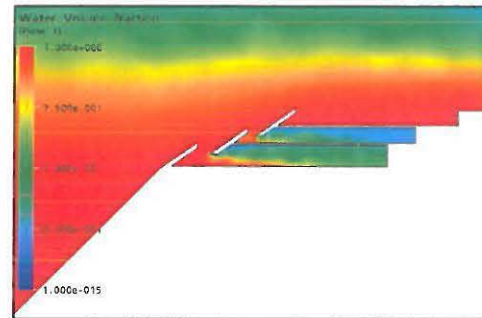


Fig. 24: WVF after 8.514s (peak pressure)

The lowest reservoir is still subjected to the highest pressure. The maximum pressure is 2.26 kPa, at scale 1:1 it corresponds to a pressure of **135.6 kPa** for a wave of height 4.8 meters.

Unlike the first computation where the water reached with difficulty in the highest reservoir, the figure 24 shows that the water flow recovers totally in the SSG model. Also the water does not enter into the closed reservoirs, the air remains inside and the reservoirs contain a mixture of air and water. This phenomenon has been already observed and chimneys have been designed to enable the air to escape. A diffusion of water is again observed and is more significant than in the last computation.

The wave amplitude is damped during the wave displacement. The water mean level seems to increase but the water volume in the fluid domain stays constant during one wave period.

Therefore the improvement of water mean level is due to the diffusion of water. This diffusion is not realistic so it is probably due to numerical approximations. A sketch (Fig. 25) has been drawn to represent what happens numerically. Each volume element is assigned by the variable of Water Volume Fraction.

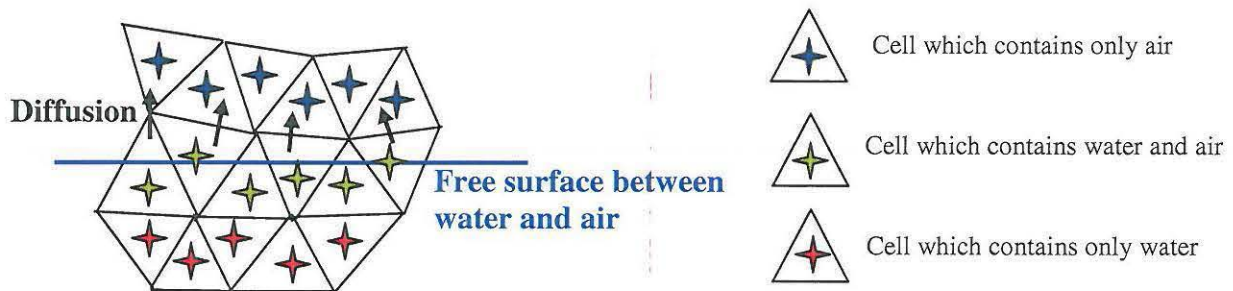


Fig. 25: Sketch of the meshes around the free surface

As illustrated in the figure 25, longer the spacing mesh, more significant the diffusion.

In order to confirm this explanation, a computation has been done by increasing spacing mesh.

c. Rougher mesh with $H=0.38$

The spacing mesh has been multiplied by 2.

Body spacing	Maximum spacing	140 mm
Face spacing (Plane 1 to 6)	Maximum spacing	5 mm
	Minimum spacing	10 mm

Table 6: Mesh spacing

The results obtained are represented below. The figure 26 shows that the meshing size has an impact on the wave damping:

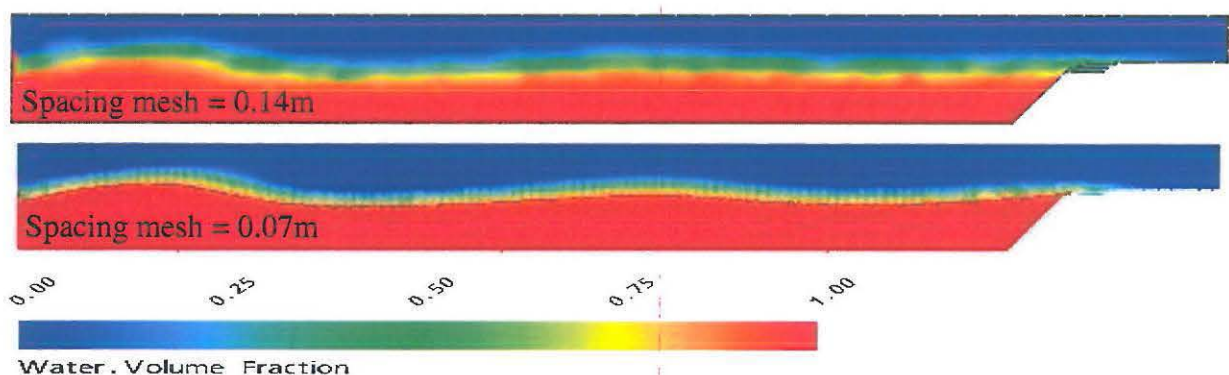


Fig. 26: Water volume fraction comparison with different meshing size (8.514 s)

The figure 27 and 28 compare the water volume fraction at the peak pressure. With a meshing size of 0.07 meters, the wave reaches the last reservoir with difficulty (Fig. 28). With a bigger meshing size, the wave does not reach the reservoirs (Fig. 27).

Moreover the isosurfaces, where the water volume fraction is equal to 0.01, 0.5 and 0.99, are presented on the figures below.

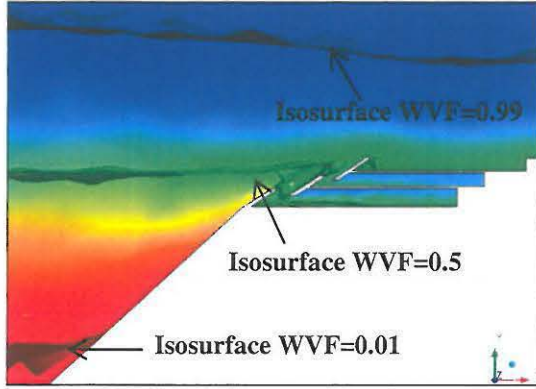


Fig. 27: Spacing mesh = 0.14 m

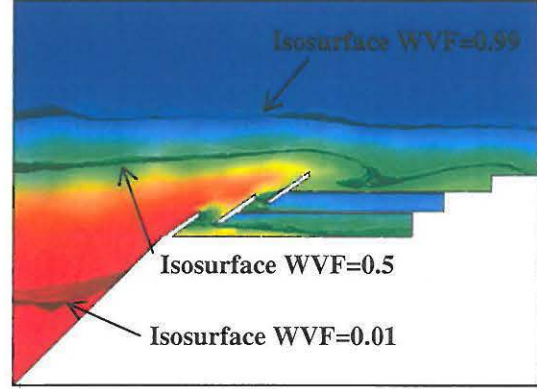


Fig. 28: Spacing mesh = 0.07 m

The heights of these isosurfaces have been reported in the figure 29:

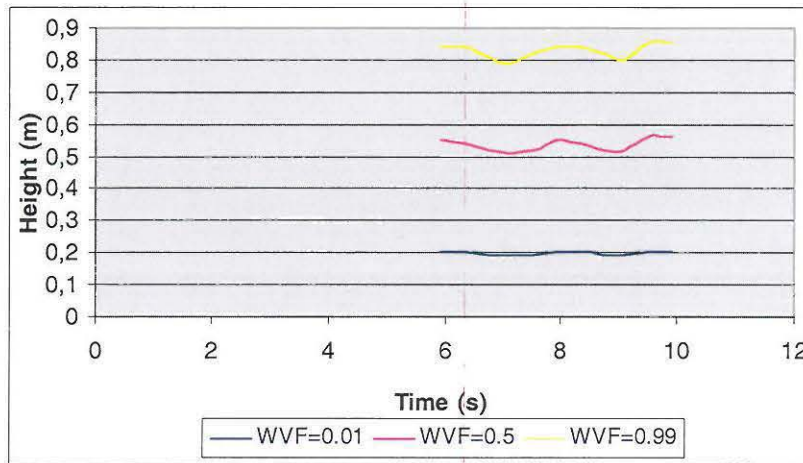
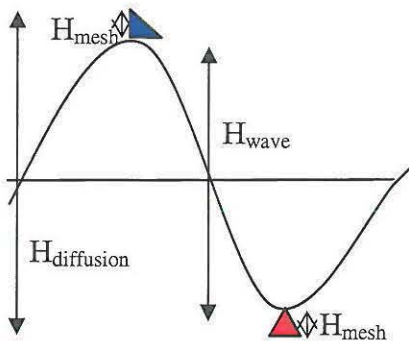


Fig. 29: Variation of the isosurfaces height during the two last periods

The height difference between the isosurface WVF=0.01 and the isosurface WVF=0.99 varies between 0.6 and 0.65 meters. So the water is diffused on a height of 0.6-0.65 meters, this height will be called diffusion height. As for a meshing size of 0.07 meters, the diffusion height is around 0.035.



The maximum diffusion height may be calculated as follows:

$$H_{\text{diffusion}} = H_{\text{wave}} + 2 * H_{\text{mesh}} \quad (\text{Eq. 24})$$

Fig. 30: Scheme of the diffusion height

A comparison for the observed diffusion height and the maximum diffusion height has been presented for spacing meshes of 0.07 and 0.14 meters in the table 7.

Meshing size	$H_{\text{diffusion}}$ observed	$H_{\text{diffusion}}$ calculated	$\frac{\text{Mesh size}}{\text{Wave height}}$
0.07	0.35	0.52	0.18
0.14	0.6-0.65	0.66	0.36

Table 7: Comparison between observed and calculated diffusion height

To reduce the diffusion height, the ratio between the mesh size and the wave height must tend to zero. It would be interesting to lead different computation with different mesh size and then to plot the diffusion height as function of mesh size.

In order to avoid this damping during the wave displacement, the length of fluid domain is reduced. This computation is presented in the next part.

d. Short model with $H=0.38$ meters

The geometry and dimensions of model structure used are defined in the first and second computation (Fig. 13). The length of the fluid domain has been reduced only (Fig. 24). Now, 0.2 meters are present between the inlet and the beginning of the slope. The mesh has been defined with the values of Table 3.

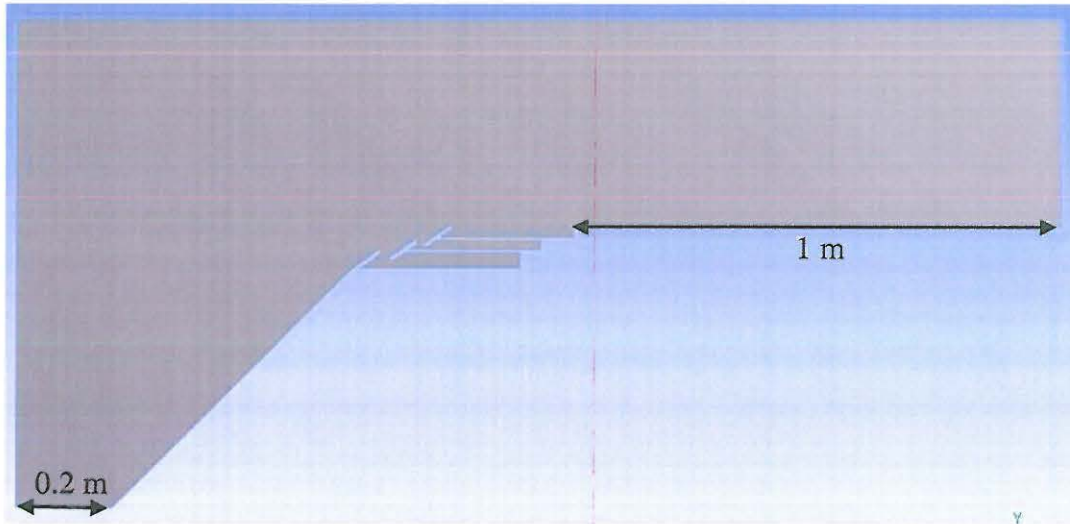


Fig. 31: Geometry of the short fluid domain with SSG model

The simulated waves have the following properties: $H_s=0.38\text{m}$ and $T=1.98\text{s}$. The surface profile is observed in the figure 32 when the velocity is positive, so when the water is going into the fluid domain. On the animation, it has been observed a significant water volume variation: the fluid domain fills and then empties. The problem of this short fluid domain is that the water volume varies a lot during one wave period due to the velocity. When the velocity is negative, the water level drops significantly. Therefore this simulation does not reflect the real conditions.

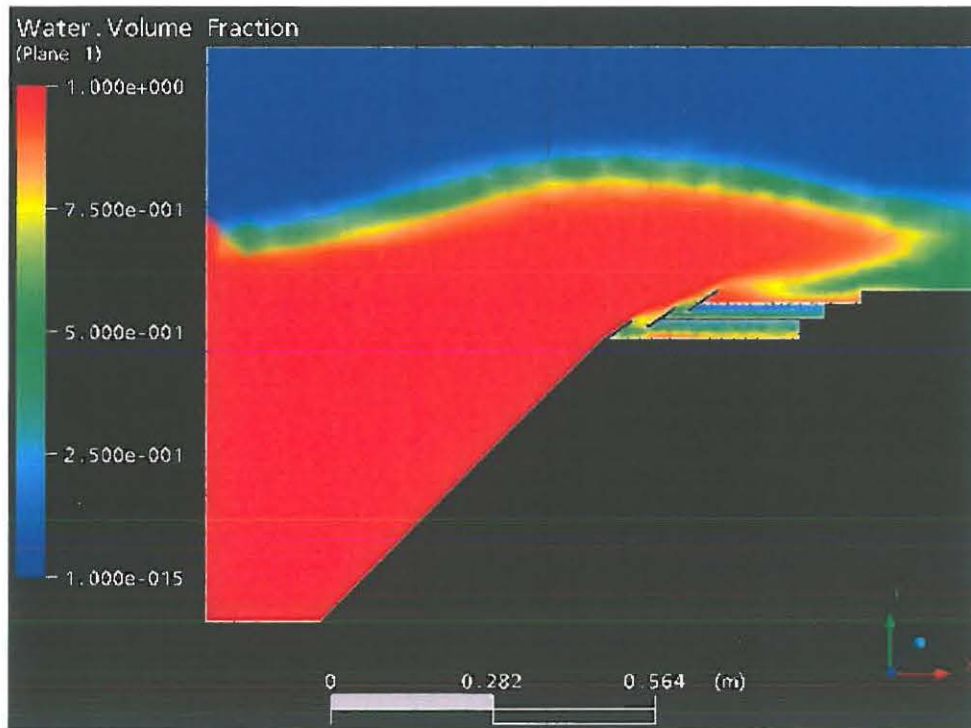


Fig. 32: Water volume fraction after 8.316s

However, as shown in the figure 32, extreme wave is created and it recovers the whole structure. The pressure on the front and back walls has been plotted:

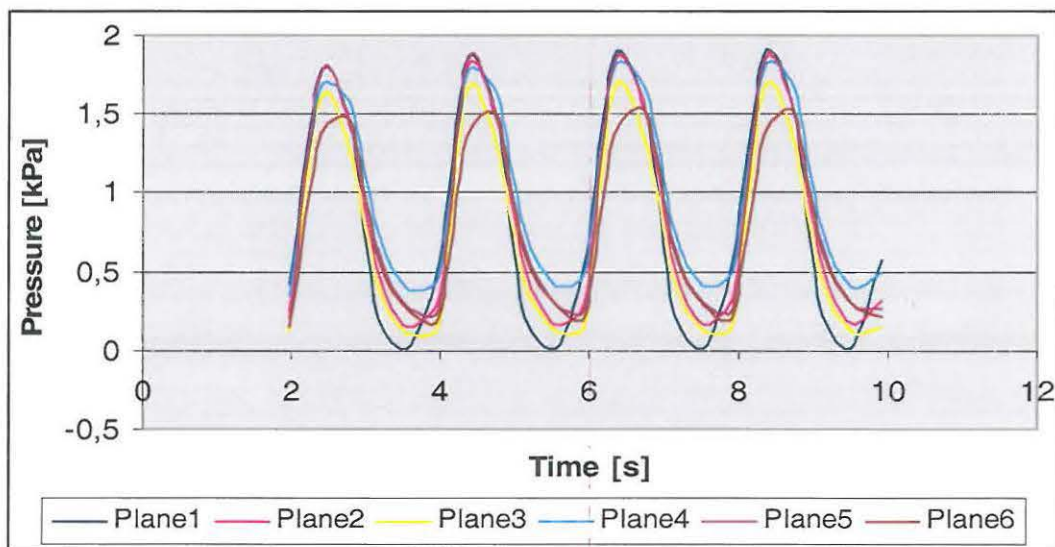


Fig. 33: Pressure time history

The highest pressure has still been recorded on plane 1 with an intensity of 1.87 kPa. At real scale, this represents a pressure of **112.2 kPa**. It is observed that Plane 1 and 5 are subject to almost the same pressure. Plane 6 stays the least loaded.

e. Conclusion on the model simulations

A diffusion of water has been observed around the free surface in the fluid domain. In order to avoid this phenomenon a fine grid should be used around the surface either with a mesh adaptation or the spacing mesh control. Also, the length of the fluid domain seems to have an influence on the diffusion. It needs to be long enough to minimize the water volume variation and short enough to limit the wave damping and the computational time.

In the model experiments done at Aalborg University, the conclusions are:

- Loads corresponding to the 100 years design wave event are for the **reservoir fronts** (Planes 1, 2 and 3) up to **190 kPa**. For the extreme peak pressure, the pressure is up to **250 kPa**.
- On the **vertical rear wall in the upper reservoir** (Plane 6), the maximum impact pressure, very peaked and short duration (Fig. 34), was equal to **580 kPa**.

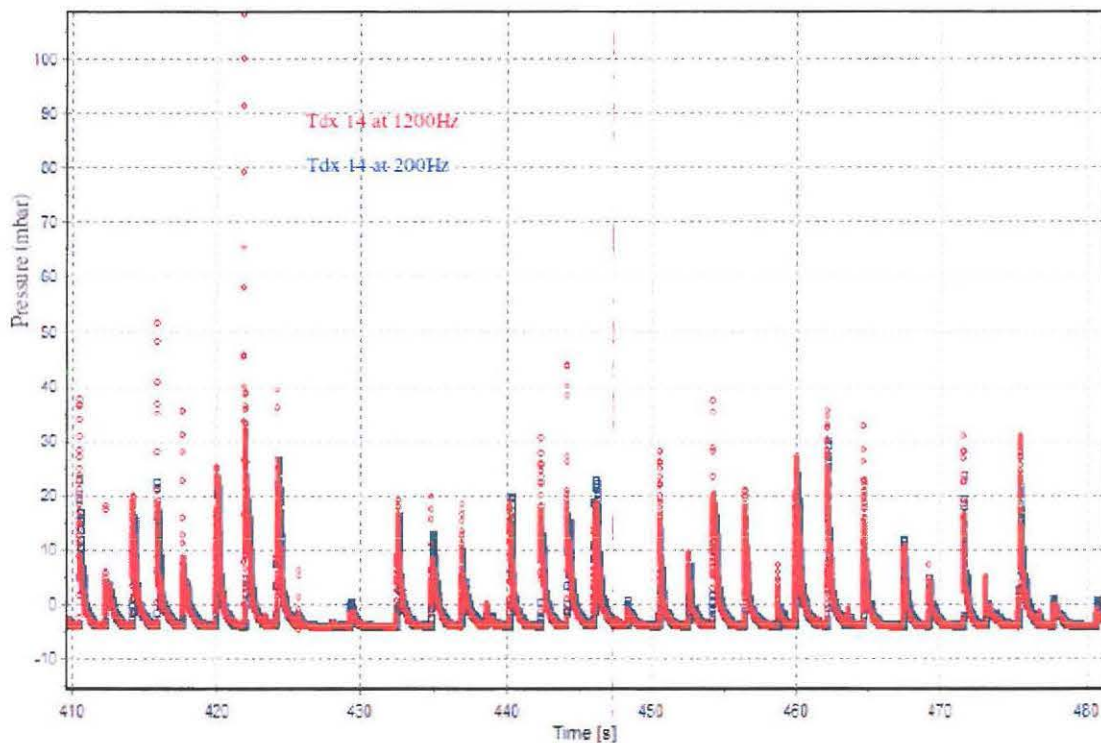


Fig. 34: Experimental results of pressure on Plane 6 time history acquired at 200Hz and at 1200Hz for transducer 14.

The computational simulation predicts lower pressure (**112.2 kPa**) in the last one for Plane 1. The plane 6 is the least loaded contrary to experimental conclusions. The difference of results may be explained with two reasons. Firstly, the sample frequency in CFD is low (transient file each 0.198 seconds so 5.05 Hz) whereas the experimental highest pressure has been recorded with a frequency of 1200Hz. Secondly, the diffusion of water due to numerical approximations makes the simulation of wave impact tough. The pressure on rear walls is smaller than the front walls because this loading is created by a mixture of air and water.

These simulations at scale 1:60 enable to try different computations because the computational time is not very long: 1 day and few hours. However the results must be compared with a simulation at full scale.

VI. Full scale under extreme wave loading

1. Geometry

The following geometry and dimensions have been used for modelizing the structure of SSG at full scale:

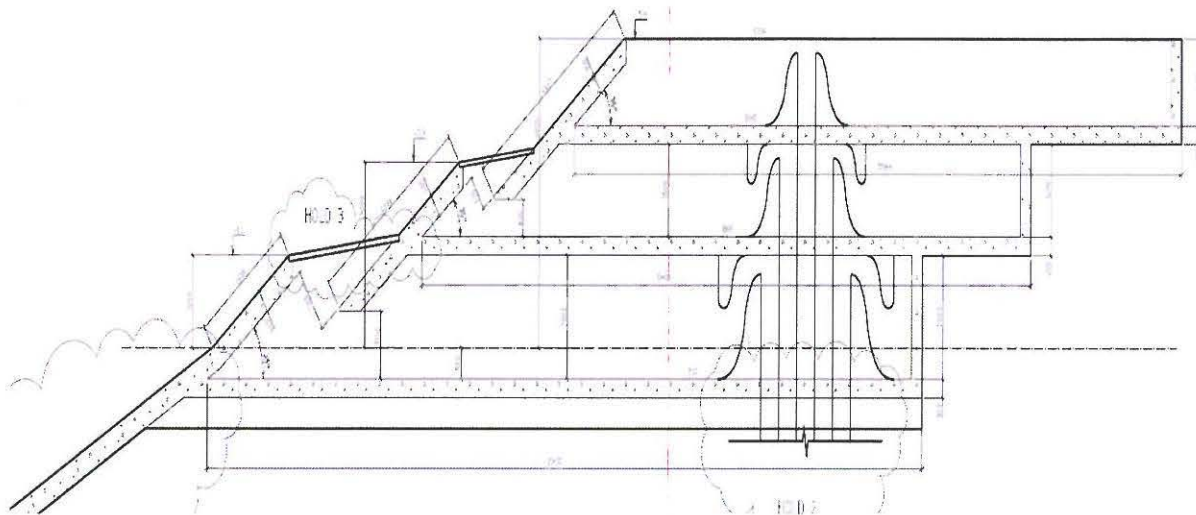


Fig. 35: Draft of the prototype structure geometry

The dimensions of the fluid domain have been presented in the figure 36. The fluid domain thickness has been limited at 0.3 meters in order to save computational memory and time. Two pipes of 5 cm radius have been modeled for preventing the air blockage in the closed reservoir (Fig. 37).

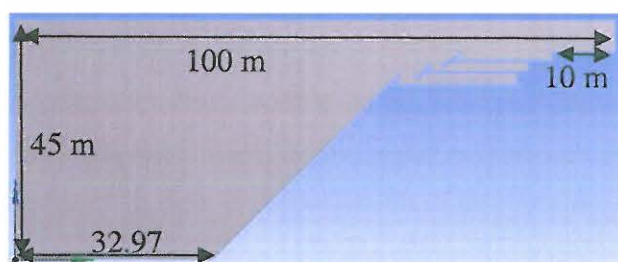


Fig. 36: Structural geometry of SSG

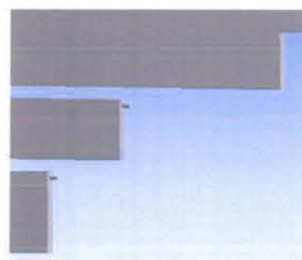


Fig. 37: Added pipes

2. Mesh

Since the thickness of the domain is 0.3 meters, the spacing mesh can not be greater than 0.3 meters.

Body spacing	Maximum spacing	0.25 m
Face spacing (Plane 1 to 6)	Maximum spacing	0.06 m
	Minimum spacing	0.03 m

Table 8: Mesh spacing for full scale

As shown in figure 38, the realized meshing is finer than the mesh of the model. The fluid domain contains 149983 nodes and 594920 volume elements.

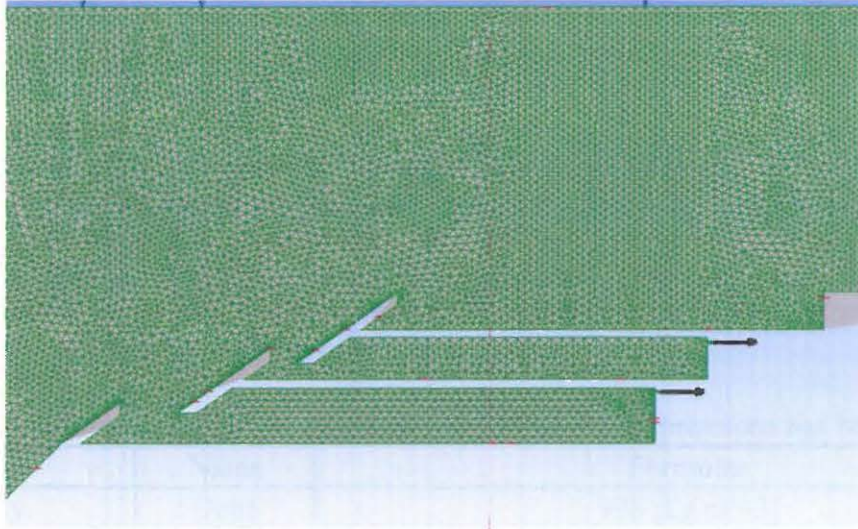


Fig. 38: Mesh for SSG at full scale, zoom around SSG

3. Wave simulation

At full scale, a wave of 23.3 meters height and 12.3 seconds period must be simulated. The following wave parameters have been calculated:

Parameters	Formulae	Values
Wave length L	$c^2 = \frac{g}{k} \tanh(kh)$	183 m
Wave number k	$\frac{2\pi}{L}$	0.0343
Period number w	$\frac{2\pi}{T}$	0.511
Propagation speed v	$\frac{L}{T}$	14.878 m/s
Velocity profile	$u = \frac{agk}{w} \frac{\cosh k(h+z)}{\cosh kh} \cos(\omega t - kx)$	$u = 4.86 \cosh 0.0343(0.5 + z) \cos(0.511t - 0.0343x)$ (Eq.2...)

Table 9: Wave parameters

In the simulation, the water level has been initialized at 30 m (Fig.39). Under this height, there is no air: Water Fraction Volume = 1, colored in red, and above only air is present: Water Fraction Volume = 0, colored in blue.

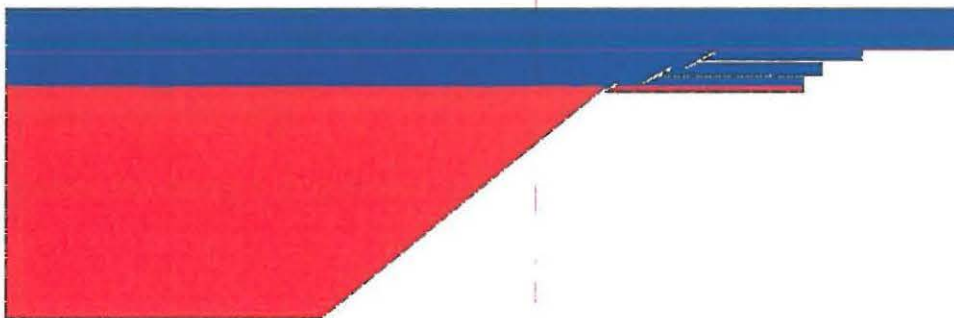


Fig.39: Water level initialization

5. Results and interpretations

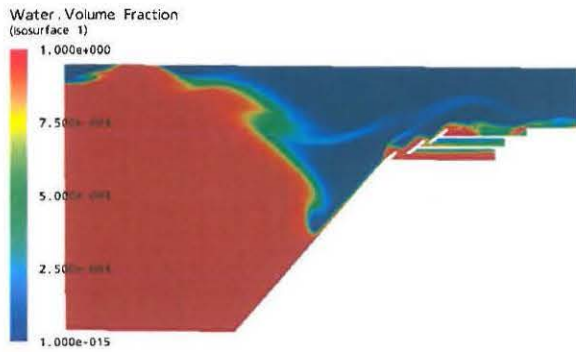


Fig. 40: WVF before peak pressure

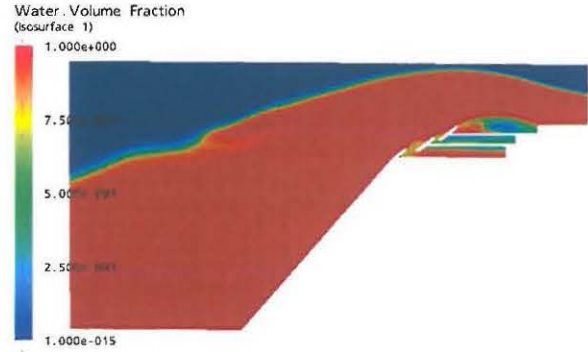


Fig. 41: WVF at 41.82 s (peak pressure)

As the fourth computation (short fluid domain), the water variation is significant during one period. The fluid domain should be extended in order to have real wave conditions. The diffusion phenomenon is less significant (Fig. 41) since the mesh is finer than for the model simulation. Here, the ratio between the mesh size and the wave height is equal to 0.01.

The averaged pressure during the last period on SSG walls has been reported in the figure 42 and the peak pressure has been presented in Table 10:

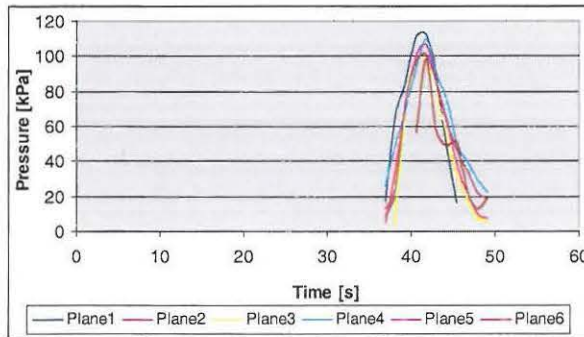


Fig. 42: Pressure during the last period

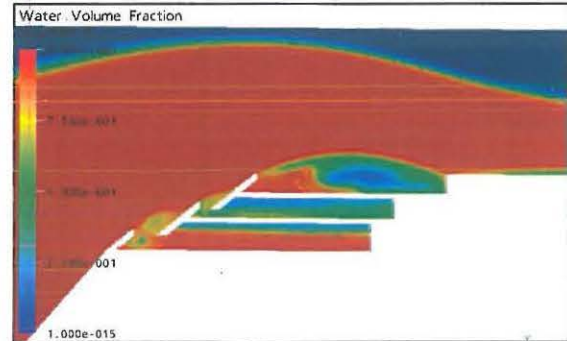


Fig. 43: WVF at 41.82 s (peak pressure), zoom

Time [s]	Plane 1	Plane 2	Plane 3	Plane 4	Plane 5	Plane 6
4.92	88.74	86	63.24	59.63	11.03	15.26
17.22	104.21	99.43	93.84	99.54	94.14	57.26
29.52	110.71	105.66	98.44	105.63	98.39	66.77
41.82	111.95	106.26	98.48	109.56	100.87	98.54

Table 11: Peak pressure for each wave period

The maximum pressure is still observed on Plane 1 with a value of **111.95 kPa**. A pressure of 112.2 kPa has been deduced from the fourth simulation (scale 1:60). The pressure magnitude is similar in the both scales therefore a small scaled simulation will be preferable for saving computational time and memory.

VII. Full scale SSG with normal waves

Simulations with extreme wave predict the wave loadings, which must be used to design the SSG structure. Moreover, simulations may be used to optimize the overtopping flow recovers by SSG. Therefore computation has been done with normal wave to know if predicted water flow is relevant.

1. Geometry and mesh

The geometry and mesh are identical as before, and there are no pipes.

2. Wave simulation

The table 12 gives the significant wave heights at the test site.

Hs, average over dir. [m]	1,3	2,9	5,2
H [m]	0,9	2,1	3,7
Tp [s]	7	9,95	12,2
Pwave [kW/m]	4,7	35,5	134,0
Prob	56,8%	24,7%	5,0%
Pwave*Prob	2,669952	8,761838	6,701443

Table 12: Probability of significant wave heights at the test site

Due to lack of time, the computation has been performed only for the wave conditions with the significant wave height of 5.2 meters. A wave of **3.7 meters** height and **9.95 seconds** period has been simulated at the inlet of the fluid domain. The following wave parameters have been calculated:

Parameters	Formulae	Values
Wave length L	$c^2 = \frac{g}{k} \tanh(kh)$	135 m
Wave number k	$\frac{2\pi}{L}$	0.046
Period number w	$\frac{2\pi}{T}$	0.63
Propagation speed v	$\frac{L}{T}$	14.07 m/s
Velocity profile	$u = \frac{agk}{w} \frac{\cosh k(h+z)}{\cosh kh} \cos(\omega t - kx)$	$u = 0.36 \cosh 0.046(0.5 + z) \cos(0.63t - 0.046)$ (Eq.2...)

Table 13: Wave parameters

As before, the water level has been initialized at 30 m. The back wall of the reservoirs has been defined as outlet in order to know the mass flow. The boundary conditions have been defined as follows:

- Inlet for the front wall
- Opening for the top

- Outlet for the back wall and the back wall of the reservoirs
- Symmetry for the side walls
- Walls everywhere else (SSG and bottom)

For simulating waves in CFX, the velocity profile at the inlet has been defined with the equation 21 that becomes at the inlet ($x = 0$): $u = 0.36 \cosh 0.046(0.5 + z) \cos(0.63t)$ (Eq.26).

To define the inlet and initialization conditions, the following expressions has been written:

Variables	Name	Formulae
Density	Dens	998 [kg m ⁻³]
Wave height initialized	H	30 [m]
Wave height at the inlet	HIn	31.85 [m]
Pressure at the inlet	InPres	$\text{dens} * g * (HIn - y) * \text{InVolWater}$
Speed at the inlet	InSpeed	$0.36 * \cosh(0.046 * Xsd) * \cos(0.63 * \text{time}) * \text{InVolWater}$ [m/s]
Air Volume Fraction at the inlet	InVolAir	$\text{step}((y - HIn) / 1[\text{m}])$
Water Volume Fraction at the inlet	InVolWater	$1 - \text{InVolAir}$
Initialized pressure	pression	$\text{dens} * g * (H - y) * \text{VolWater}$
Time variable dimensionless	time	$t / 1[\text{s}]$
Initialized Air Volume Fraction	VolAir	$\text{step}((y - H) / 1[\text{m}])$
Initialized Water Volume Fraction	VolWater	$1 - \text{VolAir}$
Height variable dimensionless	Xsd	$y / 1[\text{m}]$

Table 14: Expressions used in CFX

3. Solver

The simulation is transient and has used a time step of 0.244 seconds; hence there are 50 time steps per period. The simulation covers 4 wave periods (48.8 seconds). A transient file has been saved every 5 time steps (1.22 seconds). The selected transient scheme option is first order backward Euler and 10 loops are done between each time step.

4. Results and interpretations

To analyze these results, several charts have been plotted for representing the water level before the slope (Fig. 44), the water mass flow (Fig. 45) which goes out through the rear walls and the pressure on the front walls (Fig. 47).

In the figure 44, the wave height is 2.5 meters, so the wave amplitude is damped. Moreover it is observed that the water level decreases. In this simulation, the water which flows in the reservoir is going out of the fluid domain, therefore there is a loss in the water volume.

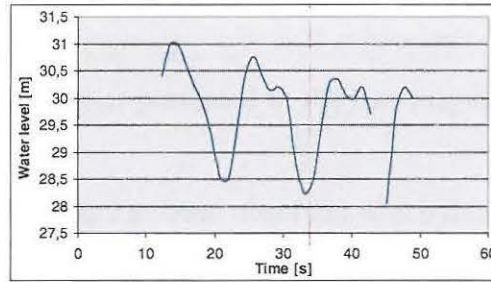


Fig. 44: Water level time history before the SSG at $x = 0.2$ meters

The water mass flow recorded is very low. In the peak mass flow, the water flow reaches 5 kg/s which represents a hydraulic power of 49.1 W. In a model testing of the SSG⁶, the hydraulic power was estimated at 6-7 kW. The hydraulic power obtained is not relevant. In the figure 46, it is observed that the flow in the reservoirs is composed of water and air. This can explain the low hydraulic power obtained in this simulation. Here, it is seen the importance of limiting the diffusion in order to have relevant results concerning the water flow.

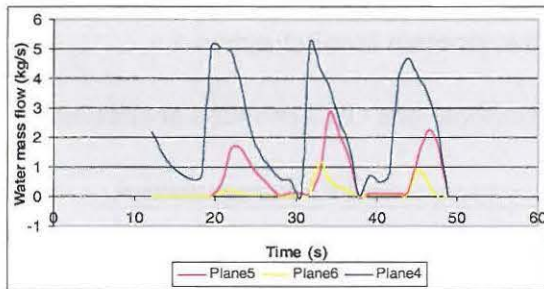


Fig. 45: Water flow mass time history through the rear walls

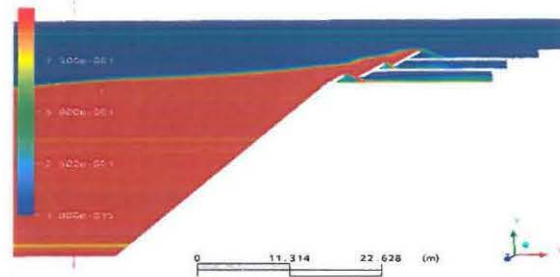


Fig. 46: Water Volume Fraction when the mass flow is the largest (28.9 seconds)

The pressure time history has been reported in the figure 47. A maximum pressure of 30.77 kPa has been found on the plane 1. In the first computation (scale 1:60), a maximum pressure of 50.16 kPa has been estimated for a wave of 3.54 meters. In this simulation, a lower pressure has been found, which is probably due to the wave damping.

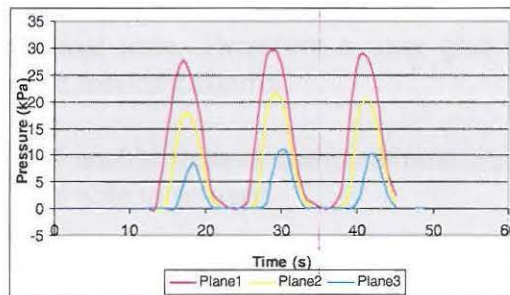


Fig. 47: Pressure time history on the front walls

As the water volume varies a lot and the results are not relevant, new computation should be carried out with a longer fluid domain and pipes to direct the output water in the domain for keeping the same water level.

⁶ J.P. Kofoed, *Model testing of the wave energy converter Seawave Slot-Cone Generator*, Hydraulics & Coastal Engineering Laboratory, Department of Civil Engineering, Aalborg University, April, 2005

IX. References

Sverdrup, Norwich oceanographer

A. Svendsen and G. Jonsson, *Hydrodynamics of coastal regions*, 1976

H.K. Versteeg & W. Malalasekera, *An introduction to Computational Fluid Dynamics*, Longman Group Ltd 1995

A.P. McCabe, *An Appraisal of a Range of Fluid Modelling Software*, Department of Engineering Lancaster University, October, 2004

Diego Vicinanza et al., Wave loadings on Seawave Slot-Cone Generator at Kvitsøy Island, Hydraulics & Coastal Engineering Laboratory, Aalborg University, March 2006.

J.P. Kofoed, *Model testing of the wave energy converter Seawave Slot-Cone Generator*, Hydraulics & Coastal Engineering Laboratory, Department of Civil Engineering, Aalborg University, April, 2005